Author's Accepted Manuscript

Comparison of two synthesis methods on the preparation of Fe, N-Co-doped TiO$_2$ materials for degradation of pharmaceutical compounds under visible light

Cinthia G. Aba-Guevara, Iliana E. Medina-Ramírez, Aracely Hernández-Ramírez, Juan Jáuregui-Rincón, Juan Antonio Lozano-Álvarez, José Luis Rodríguez-López
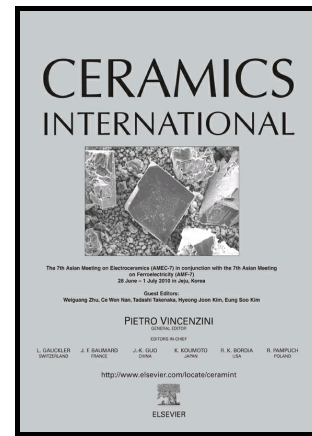
Cite this article as: Cinthia G. Aba-Guevara, Iliana E. Medina-Ramírez, Aracely Hernández-Ramírez, Juan Jáuregui-Rincón, Juan Antonio Lozano-Álvarez and José Luis Rodríguez-López, Comparison of two synthesis methods on the preparation of Fe, N-Co-doped TiO$_2$ materials for degradation of pharmaceutical compounds under visible light, *Ceramics International*, http://dx.doi.org/10.1016/j.ceramint.2017.01.018

Comparison of two synthesis methods on the preparation of Fe, N-Co-doped TiO₂ materials for degradation of pharmaceutical compounds under visible light

Aba-Guevara, Cinthia G.[1], Medina-Ramírez, Iliana E.[1,*], Hernández-Ramírez, Aracely[2],

Jáuregui-Rincón, Juan[3], Lozano-Álvarez Juan Antonio[3], Rodríguez-López José Luis[4].

[1]Departamento de Química, Universidad Autónoma de Aguascalientes. Av. Universidad # 940, Ciudad Universitaria, C.P. 20131, Aguascalientes, Ags., México.

[2]Universidad Autónoma de Nuevo León. Facultad de Ciencias Químicas. Guerrero y Progreso s/n, Col. Treviño. Monterrey, Nuevo León, México. C. P. 65570

[3]Departamento de Ingeniería Bioquímica, Universidad Autónoma de Aguascalientes. Av. Universidad # 940, Ciudad Universitaria, C.P. 20131, Aguascalientes, Ags., México.

[4]Advanced Materials Department, Instituto Potosino de Investigación Científica y Tecnológica, A.C. Camino Presa Sn José 2055, Lomas 4ª Secc., 78216 San Luis Potosí, SLP, México.

[*]Correspondence should be addressed to Iliana E. Medina-Ramírez; iemedina@correo.uaa.mx

Abstract

In this work, we report the synthesis, characterization and photocatalytic evaluation of visible light active iron-nitrogen co-doped titanium dioxide (Fe^{3+}-$TiO_{2-x}N_x$) nanostructured catalyst. Fe^{3+}-$TiO_{2-x}N_x$ was synthesized using two different chemical approaches: sol-gel (SG) and microwave (MW) methods. The materials were fully characterized using several techniques (SEM, UV-Vis diffuse reflectance DRS, X-ray diffraction XRD, and X-ray photoelectron spectroscopy XPS). The photocatalytic activity of the nanostructured materials synthesized by both methods was evaluated for the degradation of amoxicillin (AMX), streptomycin (STR) and diclofenac (DCF) in aqueous solution. Higher degradation efficiencies were encountered for the materials synthesized by the SG method, for instance, degradation efficiencies values of 58.61 % (SG) and 46.12 % (MW) were observed for

AMX after 240 minutes of photocatalytic treatment under visible light at pH 3.5. With STR the following results removal efficiencies were obtained: 49.67 % (SG) and 39.90 % (MW) at pH 8. It was observed the increasing of degradation efficiencies values at longer treatment periods, i.e., after 300 minutes of photocatalytic treatment under visible light, AMX had a degradation efficiency value of 69.15 % (MW) at pH 3.5, DCF 72.3 % (MW) at pH 5, and STR 58.49 % (MW) at pH 8.

Key words: Photocatalysis, wastewater treatment, microwave assisted synthesis, co-doped Fe^{3+}-$TiO_{2-x}N_x$ catalyst, sol-gel method.

1. Introduction

The presence of numerous ubiquitous pollutants in the environment, result in environmental degradation and in deleterious effects on the health of living organisms, including human beings. Thus, affordable and sustainable technologies for environmental remediation should be developed and implemented.

Advanced Oxidation Processes (AOPs) have demonstrated to be an efficient and affordable option for the tertiary treatment of aqueous effluents due to their strong and unspecific capacity to oxidize organic matter (Zuorro et al. 2013). Among these AOPs, TiO_2 photocatalysis has been shown to be an environment friendly technique that deeply oxidize and significantly mineralize persistent water contaminants (Vaiano et al. 2014).

Titania (TiO_2) as a photocatalyst is widely used for decomposition of toxic organic compounds. But its practical applications are still limited because of the material´s band gap value (3.2 eV) and the high degree of charge carrier recombination (Bakar and Ribeiro 2016; Asahi et al. 2014). The use of non-metal doping has been considered within the last ten years as a promising way to modify the photo-absorption properties of TiO_2 for harvesting visible light (Asahi et al. 2014).

Among non-metal dopants, nitrogen dopant offers several advantages due to the similarity on chemical properties compared to oxide ion, abundance, high variety of precursors and low cost. Besides being visible light sensitive, some nitrogen doped TiO_2 materials exhibit enhanced photocatalytic activity (Shao et al. 2008). Table 1 summarizes important contributions related to the synthesis, characterization and applications of N-TiO_2 doped materials.

Recently, two review articles regarding the synthesis, characterization and practical applications of $N-TiO_2$ and N-codoped-TiO_2 were published (Bakar and Ribeiro 2016; Asahi et al. 2014). In these publications, the enhanced photocatalytic activity of $N-TiO_2$ materials is highlighted. To date, the materials can be fabricated with different compositions, morphologies and topologies (spheres, nanotubes, nanowires, nanorods, powders, thin films). Although the material has been widely studied, still the origin of visible light activity is debated. Also, rapid, robust and reproducible techniques for the large scale production of efficient $N-TiO_2$ materials are still being sought.

  Some $N-TiO_2$ co-doped materials have also been reported in the literature. For instance, Cong Ye (2007) et al., described the synthesis, characterization and photocatalytic evaluation of Fe, $N-TiO_2$ materials. The materials were prepared by a precipitation—hydrothermal method that allowed incorporation of the dopants into the TiO_2 lattice. The materials exhibited enhanced photocatalytic activity for the degradation of Rhodamine B. It is important to remark that despite the many publications regarding $N-TiO_2$ materials, there are very few studies with respect to their application for the mineralization of emergent pollutants in water. For instance, $Cr^{3+},N-TiO_2$ exhibited good photocatalytic activity for the degradation of lindane (Senthilnathan and Philip 2010).

In this work, we are interested on the optimization of a synthetic pathway for the production of $Fe^{3+},N-TiO_2$ codoped materials with enhanced photocatalytic activity for the removal of pharmaceutical compounds (PCs) from water. Previous studies from our group indicate that the sol-gel method is a reliable technique for the production of metal doped TiO_2 materials (Pan et al. 2010; Medina-Ramírez et al. 2014; Hernandez-Ramírez and Medina-Ramírez 2015; Medina-Ramirez et al. 2011; Garcidueñas-Piña et al. 2016). In view of these results, in this study we are interested on the optimization of a microwave assisted technique for the production of visible light active TiO_2 materials. Despite the many advantages on the use of a sol-gel method for the production of TiO_2 nanostructured materials, it is a slow process for the large scale preparation of the materials (G. Zhang et al. 2014). In this regard, the use of microwave radiation greatly reduces the time and energy consumption involved on the production of inorganic nanostructured materials. It has also been reported that the use of MW radiation contributes to the production of materials with improved properties (Bilecka et al. 2008; Raji and Palanivelu 2011; Coromelci-Pastravanu et al. 2014; Sajjia et al. 2010).

In recent years, PCs have also been considered as emerging environmental contaminants under the category of pharmaceuticals and personal care products (PPCPs) (Zhang et al. 2013). There are many concerns regarding the presence of PCs in the environment, since these compounds are bioactive and it has been observed that exert several toxic effects to living organisms (Tetreault et al. 2011).

Among all the chemical categories related to PCs, antibiotics are one of the most relevant due to their extensive use and their ubiquitous nature as environmental contaminants. Apart from many other noxious effects, the presence and uncontrolled disposal of antibiotics in the environment, may also accelerate the development of antibiotic resistance genes into bacteria, which represents health risks to humans and animals (Michael et al. 2013). Amoxicillin (AMX) is one of the most used antibiotics with an impact for the environment since is widely applied in human and veterinary therapeutics. AMX is a semi-synthetic penicillin with a beta-lactam ring able to inhibit the synthesis of bacterial cell wall (Ay and Kargi 2010). Streptomycin (STR) belongs to the group of aminoglycoside antibiotics, it is a first line compound in veterinary medicine (Du et al. 2013; Vragović et al. 2011) and it is used in the treatment of tuberculosis (Orgován and Noszál 2012). Antibiotics may be disseminated into the environment from human and agriculture sources, including excretion, discharge from wastewater treatment facilities and others (Kümmerer 2009; Sarmah et al. 2006).

On the other hand, Non-Steroidal Anti-Inflammatory Drugs (NSAIDs) have been classified as one of the most frequently group of PCs detected in aquatic environments (Mehinto et al. 2010). The NSAID diclofenac is a widely used human and veterinary PC prescribed as analgesic and anti-inflammatory agent. On the other hand, several harmful effects in aquatic ecosystems have been observed due to the subchronic exposure to environmental concentrations of diclofenac (Shao et al. 2008)

Pharmaceuticals residues can be found in all Wastewater Treatment Plants (WWTPs) effluents, due to their low removal efficiency by conventional systems (Homem and Santos 2011; Verlicchi et al. 2010). The difficulties in removing these compounds result as a consequence of their complex chemical structure and their amounts in the environment (concentrations are found in the range from 10^{-3} to 10^{-6} mg L^{-1}) which are smaller than those of conventional macropollutants encountered in wastewaters effluents (Verlicchi et al. 2012), thus, efficient technologies for the removal of these pollutants should be developed.

In the present study, $Fe^{3+}TiO_{2-x}N_x$ nanostructured powders were synthesized and fully characterized. PCs, such as AMX, STR and diclofenac were degraded using the co-doped catalyst in the presence of visible light. In general, the materials obtained through the sol-gel (SG) method showed higher degradation efficiencies in comparison to the materials produced by the microwave (MW) method.

2. Materials and methods

2.1. Synthesis of Fe^{+3}-$TiO_{2-x}N_x$ nanoparticles

2.1.1. Synthesis of Fe^{+3}-$TiO_{2-x}N_x$ nanoparticles by sol-gel method

In the first stage, an acetic acid solution of ferric nitrate was prepared by adding $Fe(NO_3)_3 \cdot 9H_2O$ (98%, Sigma-Aldrich) in glacial acetic acid at room temperature, under continuous stirring. The amount of $Fe(NO_3)_3 \cdot 9H_2O$ was adjusted until a molar ratio Fe/Ti of 0.5:95.5 was reached. Subsequently, titanium isopropoxide (TIIP) $C_{12}H_{28}O_4Ti$ (97%, Sigma-Aldrich) was dropwise added into the glacial acetic acid solution. In a different flask, 30% Arabic gum (Golden bell) solution was prepared in deionized water, this solution was stirred for 30 minutes at 60°C, and then allowed to cool. Known amounts of ammonium chloride (sigma-Aldrich) were added to the resultant Arabic gum solution at room temperature. Afterward this solution was added dropwise to the TIIP solution at room

temperature under constant stirring. To ensure a complete hydrolysis of TIIP, the solution mixture was continuously stirred for about 10 h at room temperature. Next the solution was dried at 120 °C. Finally, the dried powders were calcined at 450 °C for 4 h in an electrical furnace (FELISA FE-360).

2.1.2. *Synthesis of Fe^{+3}-$TiO_{2-x}N_x$ nanoparticles by microwave radiation*

For the microwave (MW) assisted synthesis, the same procedure followed for SG method was applied except that hydrolysis of the TIIP solution mixture was conducted under MW radiation. The mixture was heated by MW irradiation with a pressure attachment for 15 minutes. The MW reactor was set at a power of 100 W and a pressure value of 300 psi. The temperature of the reaction system was adjusted to 120 °C. After MW treatment, the solution was dried and calcined at the same conditions described above.

2.2. *Characterization of co-doped TiO_2 nanoparticles*

The samples were characterized by X-Ray Diffraction technique (XRD, SIEMENS D-5000 model VPCEA40EL) to investigate crystalline structure of the samples. The 2θ angular regions between 0 and 90° were explored at a scan rate of $1°$ s^{-1}. Crystallite size was calculated using the Scherrer's formula, $d = 0.9\lambda/\beta \cos \theta$ where λ is the incident wavelength (Cu K α = 1.5406 Å), β = full width at half-maximum (FWHM) and θ = angle of reflection.

Scanning electron microscopy (SEM, JEOL model JSM-671F) was used to investigate the morphology, size and size distribution of the samples. UV-Vis diffuse reflectance spectra were recorded in the ultraviolet-visible spectra region using a Thermo-Fisher Scientific Evolution 300 spectrophotometer equipped with an integrating sphere assembly. From the UV-Vis spectra and Kubelka-Munk theory, the bandgap (Eg) values were obtained using

$$F(R) = \frac{(1-R)^2}{2R} , \qquad\qquad\qquad\qquad \text{Eq. (1)}$$

Where R is reflectance and $F(R)$ is proportional to the extinction coefficient (α). The basic Kubelka-Munk model assumes the diffused illumination of the particulate coating. A modified Kubelka-Munk function can be obtained by multiplying the $F(R)$ function by hv using the corresponding coefficient (n) associated with an electronic transition as follows: $(F(R)*hv)^n$, n=2 for an indirect allowed transition (plotted as a $(hv)^{1/2}$ versus E in eV) .

The specific surface area (SSA) of the catalysts was determined via nitrogen-adsorption-desorption isotherms measurements at 77 K using a Quantachrome Autosorb-1 instrument. In order to better understand the stability and surface electrostatic charge of the suspended materials, zeta potential values were determined in aqueous solution at different pH values (3.5, 7, 8 and 9.5), using a Zetasizer apparatus (Malvern Instruments, Southborough, MA, USA).

X-ray photoelectron spectra of the samples were obtained using two XPS systems, i.e., a PHI 5000 VersaProbe II using a monochromatic Al Kα radiation source, with X-ray energy of 1486.6 eV and scanning speed of 0.2 eV. The beam voltage was 15 kV, with a power of 25 W and spot beam size of 100 μm. The second system was a Thermo-Scientific K-alpha+ with integrated MAGCIS detector and also with a monochromatic Al Kα radiation source, pass energy of 20 eV, 25 scans at scanning speed of 0.1 eV and spot beam size of 400 um. All X-ray spectra analysis were processed using the software Multipak^R v9.0.5.8, providing evidence of composition, chemical species and oxidation state of the dopants (N and Fe).

2.3 Evaluation of Photocatalytic Performance

Photocatalytic activities of Fe^{+3}-$TiO_{2-x}N_x$ nanostructured powders were evaluated on the degradation of AMX, STR and DCF (all the compounds were from Sigma Aldrich). 0.1 g of photocatalyst was added to 0.1 L of AMX, STR or DCF individual solutions with starting concentration of 30 mg L^{-1}. A visible light lamp was used (23 W, Westinghouse #37813), with transmission of wavelengths above 400 nm. The solutions were continuously bubbled with air under magnetic stirring.

Prior to the photocatalytic treatment, each reaction mixture (catalyst + PC solution) was stirred in the dark for 60 minutes to reach adsorption equilibrium of PC onto the photocatalyst surface. Every photocatalytic experiment was done by triplicate; reproducibility of the results was expressed as mean values including each standard deviation (SD) as a measure of dispersion (average ± SD).

The pH solution was adjusted at different pH values (3.5, 7 and 9.5 for AMX and 3.5, 7 and 8.0 for STR) using HCl and/or NaOH (0.1 M). The residual antibiotic concentration in each experiment was determined by: i) UV-Vis spectroscopy (Thermo Scientific Helios Omega Uv-Vis) and (ii) High Performance Liquid Chromatography (HPLC) (YL9100 HPLC System) at 230 nm for AMX. The data was recorded by Clarity software. The column was Luna C18 (250 mm x 4.6 mm, 5 μm). The mobile phase was 60% acetonitrile and 40% ultrapure water at a flow rate of 1 mL/min. The drug mineralization percentage was determined by Total Organic Carbon (TOC) content in a Shimadzu TOC-VCSH equipment.

3. Results and Discussion

3.1. Synthesis and characterization of Fe^{+3}-$TiO_{2-x}N_x$ samples

In this work, one of our goals was to develop nano-particles of TiO_2 co-doped with Fe and N by two synthesis methods: SG and MW. In addition, we studied these nanomaterials with the aim to establish the difference within their physicochemical properties, as a result of the method of synthesis, in particular, the effect of MW radiation on the properties of the materials.

The macroscopic properties of the materials (color, appearance, texture) are very similar independent of the method of synthesis and also, both methods showed high reaction yields: 86.02 % (SG) and 82.80 % (MW), respectively. We previously reported on the use of a sol-gel method for the synthesis of Fe^{3+}-TiO_2 materials (Medina-Ramírez et al. 2014). The main advantage of the sol-gel method is the homogeneous mixing at the molecular level of the components of a binary or ternary material, which allows the incorporation of the dopants within the polycrystalline matrix of the material (Zaleska 2008; Hernandez-Ramírez and Medina-Ramírez 2015).

However, using the SG method, to dope TiO_2 with N, can be unfavorable, since the added nitrogen, might be lost by volatilization during the process. Thus, closed systems seem to be more favorable to achieve N doping on TiO_2. In this report, we evaluated the use of a closed system activated by microwave radiation for the preparation of Fe, N co-doped TiO_2 materials.

Microwave heating techniques have been extensively used for high temperature preparation of various materials. They exhibit several main advantages over conventional heating techniques/processes, including the following: 1) they can greatly diminish the heating temperature and reduce the reaction time, 2) a uniform heating can be achieved at

molecular level, 3) heating is generated inside the sample itself via its interaction with microwaves, resulting in much enhanced heating and cooling rates and 4) the heating processes are overall more energy-saving (Cao et al. 2015).

As expected, by using microwave to carry out the synthesis of nanoparticles of TiO_2 co-doped with Fe and N, the time of synthesis was reduced from 15 hours to 4.2 hours, and further analysis demonstrate that these materials exhibit small decrease in particle size (7.09 nm MW and 7.72 nm SG). The physicochemical properties of the nanoparticles are summarized in table 2.

The particle size and crystallinity are important properties that influence in the photocatalytic activity of the catalysts and can be modulated by doping (type and amount of dopants) (Ohtani et al. 2010). Figure 1 shows XRD patterns of the obtained samples. The diffraction patterns of these materials demonstrate the crystalline nature and purity of the studied materials. It was found that anatase is the major crystalline phase for all of the prepared samples, without significant difference in regard of the synthetic method (SG or MW). No characteristic peaks were detected for Fe, N or any impurities. The absence of the diffraction peaks of iron (Fe_2O_3) or nitrogen (N_xO_y) oxides is not conclusive with respect of them being absent in the materials; it might be possible the presence of these oxides but at concentrations below of the detection limit for XRD.

The crystallite size of the materials was determined by using the Scherrer equation. A crystal size of 7.09 nm and 7.72 nm were encountered for the catalyst prepared by the MW and SG method respectively. Fe^{+3}-$TiO_{2-x}N_x$ co-doped nanoparticles exhibit slightly smaller size than Fe^{3+}-TiO_2 1% (8.95 nm) single doped materials (Medina-Ramírez et al. 2014).

The reduction on the crystallite size of the materials is due to the incorporation of dopants (Fe, C and N) within the structure of TiO_2. Dopants incorporation was confirmed by XPS analysis.

The elemental composition of the materials, encountered by XPS analysis, indicates the presence of all the proposed elements (Ti, O, N, Fe) in the materials and some adventitious contaminants (Na and C). The atomic percentage of the constituent elements varies from the MW and SG methods materials as follows: O (53.3%MW, 49% SG), Ti (24.1%MW, 18% SG), C (12.8%MW, 25.8% SG), Na (8.9%MW, 6% SG), N (0.6%MW, 0.5% SG) and Fe (0.2% MW, 0.7% SG). Due to the amount of carbon incorporation, this dopant is responsible of the lower Eg value encountered for the SG prepared materials. Also, C incorporation is responsible of visible light activity since this element is present at higher concentrations in comparison to N or Fe dopants.

The difference in the atomic ratios of Ti, O and C encountered within the materials prepared by SG an MW approaches can be explained due to the incorporation of carbonaceous species in the surface of the catalyst due to incomplete decomposition of Ti precursors and polymer surfactant. The amount of carbonaceous species incorporated into de surface of TiO_2 materials prepared by SG method is greater since the thermal treatment was not sufficient to remove the titanium precursor's ligands. Several authors have reported on the incorporation of carbon during the preparation of N-doped TiO_2 materials (Sathish et al. 2005; Mitoraj and Kisch 2008; Ahmmad et al. 2010; Aziz et al. 2012; Cheng et al. 2012). It has also been reported that thermal treatment of TiO_2-N, C at temperatures higher of $600^{o}C$, results in a decreased photocatalytic activity of the materials under visible light

due to the loss and/or modification of the carbonaceous species present in the surface of the catalyst.

A more careful examination of the atomic ratios encountered for the materials reported in this study, indicate that for MW prepared materials, empirical formula (considering Ti/O ratios from XPS analysis) results as $TiO_{2.2}$, whereas for the SG materials, the formula is $TiO_{2.7}$, which is in agreement with the higher ratio of carbon for the SG prepared materials. A higher amount of oxygen is not necessarily present within the lattice of TiO_2 material, but it is present as a form of carbon oxide on the surface of the material. Also, adsorption of carbon oxides due to exposition of the materials to the atmosphere contributes on the modification of the molar ratio of this element. Although XPS analysis involves vacuum treatment of the sample in order to remove adsorbed species on the surface of the catalyst, not always sample preparation time allows for the removal of all the chemical species present on the surface of the material.

The morphology of the catalysts and their mean particle sizes were analyzed by scanning electron microscopy (SEM). Low and high-magnification scanning electronic micrographs of the materials are presented in Figure 2. The low-magnification images clearly show that agglomerates are composed of a large number of very small spherical particles. The high magnification SEM micrographs of the samples illustrate that the particles are uniform in size, with diameter values in accordance with those calculated by the Scherrer equation. Besides composition, there are not considerable differences in properties such as crystallinity (anatase), morphology (spheres) and particle size (7-09 or 7.72 nm) among the different studied materials.

From the UV-Vis spectra (Figure 3) and Kubelka-Munk theory, the bandgap (Eg) values were obtained (Cordero-García et al. 2016) : being ~2.53 eV for (SG) and ~3.00 eV for (MW). The co-doped material prepared by the SG method exhibits a considerable reduction in its Eg value (in comparison to bare TiO_2) which evinces the activity under visible light of this material. As previously discussed, the differences encountered for Eg values are due to the amount of incorporated carbon into the materials. Although some previously published studies indicate a reduction on the Eg value due to incorporation of dopants into the TiO_2 structure (substitutional and/or interstitial), it is difficult to compare the results discussed in this work with previously published ones, since not many authors indicate the chemical composition of the material. For instance, Diker H (2011) et al reports on Eg values ∼ 2.0 eV for N-TiO_2 materials, however, the amount of nitrogen incorporated into the materials is not discussed, neither an analysis of impurity (such as carbonaceous species) incorporation is presented.

The SSA for the Fe^{+3}-$TiO_{2-x}N_x$ synthetized by SG was 103.1 m^2 g^{-1}, and from Fe^{+3}-$TiO_{2-x}N_x$ synthetized by MW was of 135.3 m^2 g^{-1}. Comparison of these results with previously published ones, indicate that the materials reported in this study, exhibit higher surface areas (Table 2). On the other hand, it has been reported that increasing the amount of iron doping, results in materials with increased SSA. For instance, iron doped (0.3, 0.5, 1.0, 2.0, 3.0 and 5%) materials prepared by SG, exhibited SSA values of 47, 26, 32, 62, 178 and 278 m^2 g^{-1} respectively (Babić et al. 2012). Also, these results are in accordance with previously published results by our group (Medina-Ramírez et al. 2014).

The stability and surface electrostatic charge properties of the materials were investigated by dynamic light scattering analysis. Results are summarized in table 3. It can be easily observed that SG prepared materials exhibit better stability (Zeta potential values $\geq$ 30 mV) and smaller size in comparison to MW produced materials. As expected the pH of the solution influences the sign of the surface charge of the materials. MW prepared materials show a negative charge at pH 7 and below, whereas SG materials are mainly, negatively charged, presenting positive charge only at low pH values (3.5). The stability of the SG prepared materials contributes to their better performance during photocatalytic degradation.

X-ray photoelectron spectroscopy was utilized to obtain information of elemental composition and oxidation states of the different elements within the samples [Figure 4 (MW) and Figure 5 (SG)]. This technique was utilized to determine elemental composition and chemical speciation, which is summarized in Table 4. The spectrum in Figure 4a shows the N1s region for the MW sample. Despite the noise, two peaks can be identified. The first peak at 399.74 eV can be attributed to the formation of Ti-O-N or to N-Ti-O bonding, both corroborating substitutional bonding for the TiO_2-xNx materials (Yoo et al. 2016; Powell et al. 2015). The second peak, situated at 402.37 eV is related to N-H bonding, which can be due to amine groups, adsorbed NH_3 or charged ammonia groups (Carbajo et al. 2011; Pietrzak 2009; Shifu et al. 2007). There is no evidence on the formation of neither N-OX ($\approx$406 eV, oxidation sates [3+] and [5+]), nor N-Ti-N bonding ($\approx$ 395-397 eV) (Shifu et al. 2007). XPS analysis of SG material (Figure 5a), shows the same overall features than that of the MW sample.

The XPS data for O1s show 4 chemical species for the microwave assisted synthesized sample (Figure 4b). Peaks at 531.35 eV are related to adventitious contamination, such as hydroxyl groups, present at the surface of nanocrystalline TiO_2 (Ti-OH) (Abdullah et al. 2016). The main peak at 529.65 eV is due to O-Ti bonding within the titanium oxide lattice in Ti_2O_3, whereas the peak at 530.32 eV, correspond to oxygen in the titanium oxide lattice for TiO_2 (O-Ti-O) (Manzo-Robledo et al. 2015; Powell et al. 2015). The data obtained from O 1s analysis is in accordance with the formation of titanium oxynitride materials, which contain Ti(III) and Ti (IV) species (Yoo et al. 2016; Pietrzak 2009).

These results were also corroborated by Ti2p XPS analysis of the samples. The peak at 528.31 eV can be related to the formation of Ti-O-N bonds in the surface of the sample, in agreement with the N1s spectrum previously shown (Powell et al. 2015). The XPS spectrum of the samples synthesized by sol-gel method shows the same signals that the microwave assisted synthesized samples (Figure 5b).

In general, chemical speciation of carbon doping can draw conflicting conclusions due to multidoping effects (Di Valentin et al). In this study, an XPS spectrum for the C1s region in the MW sample exhibits three main signals (Figure 4c): the first peak at 284.7 eV corresponds to C-C bonds from normal adventitious contamination (Shi et al. 2015; Yun et al. 2012; Qi et al. 2014; Zarrabiet al. 2005). The second one at 286.09 eV corresponds to C-OH and C = O species, which corresponds to C incorporation in the interstitial sites of the titania lattice (Shi et al. 2015; Yun et al. 2012; Qi et al. 2014; Zarrabiet al. 2005; Shi et al. 2015) The third peak at 288.40 eV is indicative of Ti-O-C=O bonding of carboxyl-like groups on the titania surface; which can be related to the substitution of titanium atoms in the lattice rather than oxygen atoms (Shi et al. 2015; Yun et al. 2012; Qi et al. 2014; Zarrabiet al. 2005; Shi et al. 2015).

The C1s region of SG materials (Figure 5c) presents a new peak at 283.97 eV which evidences the formation of O-Ti-C bonds in the titania lattice, related to the substitution of the oxygen atoms in the lattice (Yun et al. 2012). The peak around 286 eV also has an increased intensity, which means greater incorporation of interstitial C into the TiO_2 lattice. As previously discussed the amount of carbon incorporation differs due to the differences on decomposition of organometallic precursors under conventional heating and/or microwave heating. In the case of SG materials, higher amounts of carbonaceous materials are deposited on the surface, whereas MW assisted route renders materials with high purity. For comparison, the elemental composition of the materials was determined by SEM-EDS analysis.

In accordance with XPS analysis, the amount of carbon incorporation in the SG prepared materials is higher than in the ones prepared by MW assisted route, although the molar ratios differ. For instance the XPS analysis indicates 12.8 and 25.8% of carbon for the MW and SG materials respectively. The amount of carbon present on the SG materials is double with respect to the MW produced materials. Analogous results were found by SEM-EDS in which the percentages are different, 5.34 and 11.07% of carbon for the MW and SG materials respectively, but still the amount of carbon present in the SG materials is double with respect to that of the MW materials. It is important to remark that both, SEM-EDS and XPS analyses do not produce information of the whole sample, but an average of the analyses of some of the particles that constitute the sample.

The spectrum for Ti2p region, for SG samples shows three sets of doublets (Figure 4d). The first doublet at 456.07-460.93 eV corresponds to N-Ti-O and O-Ti-O-N bonding, for Ti (III) (Powell et al. 2015; Qin et al. 2015; Chisaka et al. 2016). The second and main doublet at 457.64-463.36 eV is related to the formation of Ti_2O_3 (Powell et al. 2015; Qin et al. 2015; Chisaka et al. 2016). However it can also be a mixed Ti (IV)/Ti (III) oxide, as it's only slightly shifted downwards to the 459-458 eV region of the pure TiO_2 (Crişan et al. 2015; Yoo et al. 2016). The third doublet at 459.12-464.84 eV (minor contribution, gray line) is related to the formation of pure Ti (IV) oxide (Qin et al. 2015; Chisaka et al. 2016).

There is however no evidence of the N-Ti-N bonds (≈455 eV), which agrees with the evidence found in the N1s spectrum. The spectrum of the samples synthesized by SG method present the same peaks that the MW samples (Figure 5d). There is a minor shift for the first and second doublets but the previously given assignations do not change. There is an increase of the doublet at 459.28 eV, related to pure Ti (IV) oxide, which is consistent with the O1s spectrum of this sample.

Finally, the spectrum for the Fe2p region of the MW samples is showed in figure 4e. A detailed description of the chemical speciation of this element is not possible due to the poor noise-to-signal ratio in this spectrum. The overall features can be related to Fe (II) and Fe (III) oxides, but the peaks are too broad, which suggests the existence of more species than just iron oxides. For instance, the incorporation of Fe into the TiO_2 structure which are supported by the signals reported in the Ti2p spectrum (Crişan et al. 2015). Similar results were obtained independent of the synthetic pathway. Slight differences on the resolution of the spectrum are due to the amount of Fe incorporation within the samples (Figure 5e).

In this work, our main goal was the interstitial incorporation of nitrogen and iron in the lattice of TiO_2 materials. However, our results indicate that the incorporation of these dopants is very low. As previously discussed, carbon doping is considerable high in comparison to Fe and N, being responsible of the visible light activity of the materials. Previously published studies indicate that TiO_2-C materials exhibit an enhanced photocatalytic activity under visible light (Di Valentin et al. 2005). In this work, carbon doping was demonstrated by XPS and SEM-EDS. Due to the amount of carbon incorporation and its inclusion as different chemical species, the prepared materials exhibit better physicochemical properties in comparison to bare TiO_2.

3.2.   *Photocatalytic degradation of amoxicillin and streptomycin*

The photocatalytic activity of the materials (Fe^{+3}-$TiO_{2-x}N_x$) was evaluated for the degradation of AMX, STR and DCF in aqueous solution (figures 6-9). AMX and STR solutions were used at a concentration of 30 mg L^{-1}. This concentration was chosen to allow the assessment of process efficiency within a measurable scale and the accurate determination of residual antibiotic, by the analysis techniques used in this project. Figure 6 depicts the degradation curves for AMX at different pH values (3.5, 7.0 and 9.5), using Fe^{+3}-$TiO_{2-x}N_x$ nanoparticles synthesized by sol-gel method as photocatalyst. It can be observed that higher antibiotic degradation can be achieved under acidic conditions (pH = 3.5). The pH of the solution was adjusted using a 0.1M HCl solution. The degradation percentages after 4 hours of photocatalytic treatment under visible light radiation were: 58.61 %, 32.29 % and 16.60 % for AMX at pH 3.5, 7 and 9.5, respectively. Degradation of

AMX was also conducted using the MW synthesized catalyst. Results are represented in Figure 7. Lower degradation values were observed for this catalyst: 46.12 %, 30.56% and 14.13 % at pH 3.5, 7 and 9.5 respectively.

The effect of pH on antibiotic degradation can be explained by taking into consideration the surface properties of the catalyst and acid-base properties of the drug. At lower pH values, electrostatic interactions of the chemical compound and catalyst are favored (Elmolla and Chaudhuri 2010). Due to the amoxicillin pK_a values (2.6, 7.4 and 9.6), this molecule is present in solution as a zwitterion at the pH value selected for its degradation, facilitating the electrostatic interaction between the pollutant and the catalyst. Degradation of AMX is favored at lower pH values due to the hydrolysis of the molecule (Elmolla and Chaudhuri 2010). In this study, acidic hydrolysis of AMX was evaluated under visible light in order to establish the contribution of this mechanism in the overall degradation/mineralization of AMX. A degradation percentage of only 1.16 % (data not shown) was encountered under these conditions, corroborating that acidic hydrolysis is not the main mechanism on the mineralization of AMX. Heterogeneous photocatalytic treatment is necessary in order to achieve high degradation efficiencies.

There are not many differences regarding the stability (∼30 mv) and hydrodynamic radius (∼ 450 nm) of the materials at pH 3.5. The only difference is the sign of the surface charge, which is negative for MW and positive for SG materials. As previously discussed, at this pH value, AMX molecule is present as a zwitterion, thus electrostatic interaction are favored despite the surface charge of the catalyst. Since the hydrodynamic radius of the materials is also similar, the differences encountered for the degradation of AMX might be regarded to the activity of the materials under visible light.

For the photocatalytic degradation of STR, higher efficiencies were obtained at basic pH values. In comparison to the basic pH value (9,5) utilized for photocatalytic treatment of AMX, the degradation of STR was conducted at different pH (8), due to the pKa values (8.29, 12.33 and 13.55) of the molecule. Figure 8 depicts the degradation curves as a function of a variable pH (3.5, 7 and 8) value. The results correspond to the degradation achieved by the Fe^{+3}-$TiO_{2-x}N_x$ nanoparticles synthesized by SG method. Degradation efficiencies were determined by UV-Vis spectrophotometry. Results indicate that after 240 min of photocatalytic treatment, degradation efficiencies were 26.80 %, 41.80 % and 49.67 % at pH 3.5, 7 and 8, respectively. Same patterns but lower degradation values were observed for the MW synthesized catalyst: 16.63 %, 32.47 % and 39.90 % at pH 3.5, 7 and 8 respectively (Figure 9 and Table 5).

Regarding the surface charge and stability of the catalyst at the pH value (8) for the degradation of STR, results indicate that MW prepared materials exhibits (+) charge, low stability and big hydrodynamic radius (752nm). Due to the positive charge on the material, electrostatic interactions between the catalyst and the STR molecule are not favored. For the SG prepared material, negatively charged species are present at pH 8, favoring the electrostatic interactions between the catalyst and STR. The SG materials exhibited higher STR degradation efficiencies in comparison to MW materials, due to favored electrostatic interactions that facilitate adsorption of the molecule to the surface of the catalyst, then its degradation. The MW synthesized catalyst was also able to degrade STR molecule, thus, adsorption of STR might be conducted through different molecular interactions. Also it is possible that release of HO· radicals to the medium initiates the degradation of the molecule, modifying its structure and possible, facilitating interaction with catalyst. Further

studies will be conducted in order to understand the mechanism for degradation of organic matter on the surface of the catalyst.

To our knowledge, very few studies on the photodegradation of STR with TiO_2 catalyst in the presence of visible light have been published. For example Ambrosetti et al. (2015) compared the activity of ZnO vs TiO_2 for the degradation of STR (50 mg L^{-1}) under UV light irradiation. Complete degradation of STR was accomplished with both materials, but higher degradation rate was observed when using TiO_2 as catalyst. It is important to remark that the materials presented in this study, were active under visible light to achieve degradation of STR, rendering a sustainable approach for the degradation of this compound.

As previously discussed for AMX, higher degradation efficiencies were achieved for STR at basic pH values due to favored electrostatic interaction between the antibiotic molecules and the catalyst surface. After adsorption, redox reactions take place, acting principally by the rupture of the aminocyclitol ring of the STR molecule (Orgován and Noszál 2012; Martínez-Mejía and Rath 2015; Sarri et al. 2006). Degradation efficiencies of 49.57% were observed after 4 hours of treatment using the SG catalyst. The higher activity observed for this material is due to the higher amount of carbon doping, since no important differences are observed within other physicochemical properties.

The degradation of DCF using Fe^{+3}-$TiO_{2-x}N_x$ nanoparticles (MW) and visible light radiation was evaluated. Mineralization was evaluated by Chemical Oxygen Demand (COD) reduction. A reduction of 72.3% on the COD value was encountered, after 5 hours

of treatment. Although, mineralization of this compound has been previously reported, (Cheng et al. 2015), using a N,S-TiO$_2$ catalyst, the time of treatment is considerable longer (12 hours) in comparison with the treatment reported in this study (5 hours).

Mineralization of antibiotics was evaluated as total organic carbon (TOC). Mineralization efficiencies of 41.51 % (AMX) and 34.72 % (STR) were obtained, after 240 min of treatment under visible light mediated by the SG catalyst. For the catalyst synthesized by microwave radiation, mineralization efficiencies were 35.99 % and 29.86 % for AMX and STR respectively. These results are in accordance with the degradation values of these molecules.

In general, the photocatalytic activity of the materials under study is better as compared to some previously published reports, since the degradation efficiencies are similar, but achieved under visible light radiation. For instance, Elmolla et al. (2010) reported the use of TiO$_2$ and UV light for the degradation of amoxicillin (AMX), ampicillin (AMP) and cloxacillin (CLX). Also, Pereira and coworkers (2014) reported on the degradation of AMX mediated by TiO$_2$ and UV light. In this study, the feasibility for degradation and/or mineralization of PCs mediated by Fe^{3+}-TiO$_2$-N,C catalyst under visible light was demonstrated. Further studies will be focused on the elucidation of the mechanism for the degradation of organic matter exerted for these materials. Also, the production of supported materials will be explored in order to facilitate their large scale applications.

4. Conclusions

Two different synthesis methods (SG and MW) were applied in the production of Fe^{+3}-$TiO_{2-x}N_x$ nanoparticles. It was observed that the amount of Fe, N and C doping is determined by the synthetic method. Carbon doping is responsible of the improvement in the properties of the studied materials and enhances the photocatalytic activity for degradation of pharmaceutical compounds in water. This work demonstrates that a sol-gel process allowed incorporation of carbon dopant in higher proportions as compared to MW assisted method. SG synthesis renders materials with highest photocatalytic activity and lower band gap. The degradation of AMX is higher when conducted at low pH values, whereas degradation of STR is higher at basic medium. Mineralization can only be achieved under those conditions. Our results indicate that the heterogeneous photocatalyst Fe^{+3}-TiO_2,N,C is effective for the degradation of amoxicillin, streptomycin and diclofenac in aqueous solutions. A sustainable technology for the tertiary treatment of hospital effluents might be developed with the use of these materials.

Acknowledgements

References

Abdullah, M., Noora J. Al-Thani, Khouloud Tawbi, and H. Al-Kandari. 2016.
"Carbon/nitrogen-Doped TiO2: New Synthesis Route, Characterization and
Application for Phenol Degradation." *Arabian Journal of Chemistry* 9 (2): 229–37.
doi:10.1016/j.arabjc.2015.04.027.

Ahmmad, B., Kusumoto, Y., and Md. Shariful Islam. 2010. "One-Step and Large Scale
Synthesis of Non-Metal Doped TiO2 Submicrospheres and Their Photocatalytic
Activity." *Advanced Powder Technology* 21 (3): 292–97.
doi:10.1016/j.apt.2009.12.009.

Arredondo Valdez, H C, G García Jiménez, S Gutiérrez Granados, and C Ponce de León.
2012. "Degradation of Paracetamol by Advance Oxidation Processes Using Modified
Reticulated Vitreous Carbon Electrodes with TiO(2) and CuO/TiO(2)/Al(2)O(3)."
Chemosphere 89 (10). Elsevier Ltd: 1195–1201.
doi:10.1016/j.chemosphere.2012.07.020.

Asahi, Ryoji, Takeshi Morikawa, Hiroshi Irie, and Takeshi Ohwaki. 2014. "Nitrogen-
Doped Titanium Dioxide as Visible-Light-Sensitive Photocatalyst: Designs,
Developments, and Prospects." JOUR. *Chemical Reviews* 114 (19). American
Chemical Society: 9824–52. doi:10.1021/cr5000738.

Ay, Filiz, and Fikret Kargi. 2010. "Advanced Oxidation of Amoxicillin by Fenton's
Reagent Treatment." *Journal of Hazardous Materials* 179 (1–3): 622–27.
doi:10.1016/j.jhazmat.2010.03.048.

Aziz, Azrina Abd, Kok Soon Yong, Shaliza Ibrahim, and Saravanan Pichiah. 2012. "Enhanced Magnetic Separation and Photocatalytic Activity of Nitrogen Doped Titania Photocatalyst Supported on Strontium Ferrite." *Journal of Hazardous Materials* 199: 143–50. doi:10.1016/j.jhazmat.2011.10.069.

Babić, Biljana, Jelena Gulicovski, Zorana Dohčević-Mitrović, Dušan Bučevac, Marija Prekajski, Jelena Zagorac, and Branko Matović. 2012. "Synthesis and Characterization of Fe3+ Doped Titanium Dioxide Nanopowders." *Ceramics International* 38 (1): 635–40. doi:10.1016/j.ceramint.2011.07.053.

Bakar, Shahzad Abu, and Caue Ribeiro. 2016. "Nitrogen-Doped Titanium Dioxide: An Overview of Material Design and Dimensionality Effect over Modern Applications." *Journal of Photochemistry and Photobiology C: Photochemistry Reviews* 27: 1–29. doi:10.1016/j.jphotochemrev.2016.05.001.

Barbara Ambrosetti, Luigi Campanella, and Raffaella Palmisano. 2015. "Degradation of Antibiotics in Aqueous Solution by Photocatalytic Process: Comparing the Efficiency in the Use of ZnO or TiO2." *Journal of Environmental Science and Engineering A* 4 (6). doi:10.17265/2162-5298/2015.06.001.

Bilecka, Idalia, Igor Djerdj, and Markus Niederberger. 2008. "One-Minute Synthesis of Crystalline Binary and Ternary Metal Oxide Nanoparticles." JOUR. *Chemical Communications*, no. 7. The Royal Society of Chemistry: 886–88. doi:10.1039/B717334B.

Cao, Yingnan, Haijun Zhang, Faliang Li, Lilin Lu, and Shaowei Zhang. 2015. "Preparation and Characterization of Ultrafine ZrB2–SiC Composite Powders by a Combined Sol– gel and Microwave Boro/carbothermal Reduction Method." *Ceramics International* 41

(6): 7823–29. doi:10.1016/j.ceramint.2015.02.117.

Carbajo, J., C. Adán, A. Rey, A. Martínez-Arias, and A. Bahamonde. 2011. "Optimization of H2O2 Use during the Photocatalytic Degradation of Ethidium Bromide with TiO2 and Iron-Doped TiO2 Catalysts." *Applied Catalysis B: Environmental* 102 (1–2). Elsevier B.V.: 85–93. doi:10.1016/j.apcatb.2010.11.028.

Cheng, Xiuwen, Pu Wang, and Huiling Liu. 2015. "Visible-Light-Driven Photoelectrocatalytic Degradation of Diclofenac by N, S–TiO2/TiO2 NTs Photoelectrode: Performance and Mechanism Study." *Journal of Environmental Chemical Engineering* 3 (3): 1713–19. doi:10.1016/j.jece.2015.06.015.

Cheng, Xiuwen, Xiujuan Yu, and Zipeng Xing. 2012a. "Characterization and Mechanism Analysis of Mo–N-Co-Doped TiO2 Nano-Photocatalyst and Its Enhanced Visible Activity." *Journal of Colloid and Interface Science* 372 (1): 1–5. doi:10.1016/j.jcis.2011.11.071.

———. 2012b. "One-Step Synthesis of Fe–N–S-Tri-Doped TiO2 Catalyst and Its Enhanced Visible Light Photocatalytic Activity." *Materials Research Bulletin* 47 (11): 3804–9. doi:10.1016/j.materresbull.2012.05.030.

Chisaka, M, Y Ando, and N Itagaki. 2016. "Activity and Durability of the Oxygen Reduction Reaction in a Nitrogen-Doped Rutile-Shell on TiN-Core Nanocatalysts Synthesised via Solution-Phase Combustion." JOUR. *Journal of Materials Chemistry A* 4 (7). The Royal Society of Chemistry: 2501–8. doi:10.1039/C5TA08235H.

Cong, Ye, Jinlong Zhang, Feng Chen, and Masakazu Anpo. 2007. "Synthesis and Characterization of Nitrogen-Doped TiO 2 Nanophotocatalyst with High Visible Light

Activity," 6976–82.

Cordero-García, A., J. L. Guzmán-Mar, L. Hinojosa-Reyes, E. Ruiz-Ruiz, and A. Hernández-Ramírez. 2016. "Effect of Carbon Doping on WO3/TiO2 Coupled Oxide and Its Photocatalytic Activity on Diclofenac Degradation." *Ceramics International* 42 (8). Elsevier: 9796–9803. doi:10.1016/j.ceramint.2016.03.073.

Coromelci-Pastravanu, Cristina, Maria Ignat, Evelini Popovici, and Valeria Harabagiu. 2014. "TiO2-Coated Mesoporous Carbon: Conventional vs. Microwave-Annealing Process." *Journal of Hazardous Materials* 278: 382–90. doi:10.1016/j.jhazmat.2014.06.036.

Crişan, Maria, Mălina Răileanu, Nicolae Drăgan, Dorel Crişan, Adelina Ianculescu, Ines Niţoi, Petruţa Oancea, et al. 2015. "Sol–gel Iron-Doped TiO2 Nanopowders with Photocatalytic Activity." *Applied Catalysis A: General* 504 (September): 130–42. doi:10.1016/j.apcata.2014.10.031.

Di Valentin, Cristiana, Gianfranco Pacchioni, and Annabella Selloni. 2005. "Theory of Carbon Doping of Titanium Dioxide." JOUR. *Chemistry of Materials* 17 (26). American Chemical Society: 6656–65. doi:10.1021/cm051921h.

Diker, Halide, Canan Varlikli, Koray Mizrak, and Aykutlu Dana. 2011. "Characterizations and Photocatalytic Activity Comparisons of N-Doped Nc-TiO2 Depending on Synthetic Conditions and Structural Differences of Amine Sources." *Energy* 36 (2): 1243–54. doi:10.1016/j.energy.2010.11.020.

Dimitrakopoulou, Despina, Irene Rethemiotaki, Zacharias Frontistis, Nikolaos P Xekoukoulotakis, Danae Venieri, and Dionissios Mantzavinos. 2012. "Degradation,

Mineralization and Antibiotic Inactivation of Amoxicillin by UV-A/TiO$_2$ Photocatalysis." *Journal of Environmental Management* 98 (May): 168–74. doi:10.1016/j.jenvman.2012.01.010.

Du, Bin, Hongyan Li, Jianwen Jin, Tiantian Wang, Yang Li, Guopeng Shen, and Xiaotian Li. 2013. "Chemiluminescence Determination of Streptomycin in Pharmaceutical Preparation and Its Application to Pharmacokinetic Study by a Flow Injection Analysis Assembly." *Spectrochimica Acta. Part A, Molecular and Biomolecular Spectroscopy* 115 (November). Elsevier B.V.: 823–28. doi:10.1016/j.saa.2013.07.007.

Elmolla, Emad S., and Malay Chaudhuri. 2010. "Photocatalytic Degradation of Amoxicillin, Ampicillin and Cloxacillin Antibiotics in Aqueous Solution Using UV/TiO2 and UV/H2O2/TiO2 Photocatalysis." *Desalination* 252 (1–3). Elsevier B.V.: 46–52. doi:10.1016/j.desal.2009.11.003.

Garcidueñas-Piña, Cristina, Iliana E. Medina-Ramírez, Plinio Guzmán, Roberto Rico-Martínez, José Francisco Morales-Domínguez, and Isidoro Rubio-Franchini. 2016. "Evaluation of the Antimicrobial Activity of Nanostructured Materials of Titanium Dioxide Doped with Silver And/or Copper and Their Effects on Arabidopsis Thaliana." *International Journal of Photoenergy* 2016. doi:10.1155/2016/8060847.

Hernandez-Ramírez, A., and I. Medina-Ramírez. 2015. *Photocatalytic Semiconductors Synthesis, Characterization, and Environmental Applications*.

Homem, Vera, and Lúcia Santos. 2011. "Degradation and Removal Methods of Antibiotics from Aqueous Matrices--a Review." *Journal of Environmental Management* 92 (10). Elsevier Ltd: 2304–47. doi:10.1016/j.jenvman.2011.05.023.

Kümmerer, Klaus. 2009. "Antibiotics in the Aquatic Environment--a Review--Part II."
Chemosphere 75 (4). Elsevier Ltd: 435–41. doi:10.1016/j.chemosphere.2008.12.006.

Liu, Shou-Heng, and Han-Ren Syu. 2013. "High Visible-Light Photocatalytic Hydrogen
Evolution of C,N-Codoped Mesoporous TiO2 Nanoparticles Prepared via an Ionic-
Liquid-Template Approach." *International Journal of Hydrogen Energy* 38 (32).
Elsevier Ltd: 13856–65. doi:10.1016/j.ijhydene.2013.08.094.

Liu, Xinlin, Peng Lv, Guanxin Yao, Changchang Ma, Pengwei Huo, and Yongsheng Yan.
2013. "Microwave-Assisted Synthesis of Selective Degradation Photocatalyst by
Surface Molecular Imprinting Method for the Degradation of Tetracycline onto
ClTiO2." *Chemical Engineering Journal* 217 (February): 398–406.
doi:10.1016/j.cej.2012.12.007.

Manzo-Robledo, A., A. Cruz López, A.A. Flores Caballero, A.A. Zaldívar Cadena,
Máximo López, and O. Vázquez-Cuchillo. 2015. "Photoelectrochemical Properties of
Sol–gel Synthesized Titanium Dioxide Nano-Particles Using Different Acids: X-Ray
Photoelectron Spectroscopy Reveals the Induced Effect of Hydrolysis Precursor."
Materials Science in Semiconductor Processing 31 (March): 94–99.
doi:10.1016/j.mssp.2014.11.020.

Martínez-Mejía, Mónica J, and Susanne Rath. 2015. "Use of Experimental Design to
Optimize a Triple-Potential Waveform to Develop a Method for the Determination of
Streptomycin and Dihydrostreptomycin in Pharmaceutical Veterinary Dosage Forms
by HPLC-PAD." *Journal of Pharmaceutical and Biomedical Analysis* 104 (February):
81–89. doi:10.1016/j.jpba.2014.11.026.

Medina-Ramírez, Iliana, Jingbo Louise Liu, Araceli Hernández-Ramírez, Cristina Romo-

Bernal, Gladis Pedroza-Herrera, Juan Jáuregui-Rincón, and Miguel A Gracia-Pinilla. 2014. "Synthesis, Characterization, Photocatalytic Evaluation, and Toxicity Studies of TiO2--Fe3+ Nanocatalyst." Article. *Journal of Materials Science* 49 (15): 5309–23. doi:10.1007/s10853-014-8234-z.

Medina-Ramirez, Iliana, Zhiping Luo, Sajid Bashir, Ray Mernaugh, and Jingbo Louise Liu. 2011. "Facile Design and Nanostructural Evaluation of Silver-Modified Titania Used as Disinfectant." JOUR. *Dalton Transactions* 40 (5). The Royal Society of Chemistry: 1047–54. doi:10.1039/C0DT00784F.

Mehinto, Alvine C, Elizabeth M Hill, and Charles R Tyler. 2010. "Uptake and Biological Effects of Environmentally Relevant Concentrations of the Nonsteroidal Anti-Inflammatory Pharmaceutical Diclofenac in Rainbow Trout (Oncorhynchus Mykiss)." JOUR. *Environmental Science & Technology* 44 (6). American Chemical Society: 2176–82. doi:10.1021/es903702m.

Michael, I, L Rizzo, C S McArdell, C M Manaia, C Merlin, T Schwartz, C Dagot, and D Fatta-Kassinos. 2013. "Urban Wastewater Treatment Plants as Hotspots for the Release of Antibiotics in the Environment: A Review." *Water Research* 47 (3). Elsevier Ltd: 957–95. doi:10.1016/j.watres.2012.11.027.

Mitoraj, D., and H. Kisch. 2008. "The Nature of Nitrogen-Modified Titanium Dioxide Photocatalysts Active in Visible Light." *Chemie International Edition* 47: 9975–78.

Nasuhoglu, Deniz, Angela Rodayan, Dimitrios Berk, and Viviane Yargeau. 2012. "Removal of the Antibiotic Levofloxacin (LEVO) in Water by Ozonation and TiO2 Photocatalysis." *Chemical Engineering Journal* 189–190 (May). Elsevier B.V.: 41–48. doi:10.1016/j.cej.2012.02.016.

Ohtani, B., O.O. Prieto-Mahaney, D. Li, and R. Abe. 2010. "What Is Degussa (Evonik) P25? Crystalline Composition Analysis, Reconstruction from Isolated Pure Particles and Photocatalytic Activity Test." *Journal of Photochemistry and Photobiology A: Chemistry* 216 (2–3): 179–82. doi:10.1016/j.jphotochem.2010.07.024.

Orgován, Gábor, and Béla Noszál. 2012. "NMR Analysis and Site-Specific Protonation Constants of Streptomycin." *Journal of Pharmaceutical and Biomedical Analysis* 59 (February): 78–82. doi:10.1016/j.jpba.2011.10.009.

Pan, Jian, and San Ping Jiang. 2016. "Synthesis of Nitrogen Doped Faceted Titanium Dioxide in Pure Brookite Phase with Enhanced Visible Light Photoactivity." *Journal of Colloid and Interface Science* 469: 25–30. doi:10.1016/j.jcis.2016.02.013.

Pan, Xubin, Iliana Medina-Ramirez, Ray Mernaugh, and Jingbo Liu. 2010. "Nanocharacterization and Bactericidal Performance of Silver Modified Titania Photocatalyst." *Colloids and Surfaces. B, Biointerfaces* 77 (1). Elsevier B.V.: 82–89. doi:10.1016/j.colsurfb.2010.01.010.

Pietrzak, Robert. 2009. "XPS Study and Physico-Chemical Properties of Nitrogen-Enriched Microporous Activated Carbon from High Volatile Bituminous Coal." *Fuel* 88 (10): 1871–77. doi:10.1016/j.fuel.2009.04.017.

Powell, Jonathan M, Jamie Adcock, Sheng Dai, Gabriel M Veith, and Craig A Bridges. 2015. "Role of Precursor Chemistry in the Direct Fluorination to Form Titanium Based Conversion Anodes for Lithium Ion Batteries." JOUR. *RSC Advances* 5 (108). The Royal Society of Chemistry: 88876–85. doi:10.1039/C5RA17258F.

Qi, Dianyu, Mingyang Xing, and Jinlong Zhang. 2014. "Hydrophobic Carbon-Doped

TiO2/MCF-F Composite as a High Performance Photocatalyst." JOUR. *The Journal of Physical Chemistry C* 118 (14). American Chemical Society: 7329–36. doi:10.1021/jp4123979.

Qin, Yuan-Hang, Yunfeng Li, Thomas Lam, and Yangchuan Xing. 2015. "Nitrogen-Doped Carbon-TiO2 Composite as Support of Pd Electrocatalyst for Formic Acid Oxidation." *Journal of Power Sources* 284: 186–93. doi:10.1016/j.jpowsour.2015.03.040.

Raji, Jeevitha R, and Kandasamy Palanivelu. 2011. "Sunlight-Induced Photocatalytic Degradation of Organic Pollutants by Carbon-Modified Nanotitania with Vegetable Oil as Precursor." JOUR. *Industrial & Engineering Chemistry Research* 50 (6). American Chemical Society: 3130–38. doi:10.1021/ie101259p.

Sajjia, M., M. Oubaha, T. Prescott, and a.G. Olabi. 2010. "Development of Cobalt Ferrite Powder Preparation Employing the Sol–gel Technique and Its Structural Characterization." *Journal of Alloys and Compounds* 506 (1). Elsevier B.V.: 400–406. doi:10.1016/j.jallcom.2010.07.015.

Sarmah, Ajit K, Michael T Meyer, and Alistair B a Boxall. 2006. "A Global Perspective on the Use, Sales, Exposure Pathways, Occurrence, Fate and Effects of Veterinary Antibiotics (VAs) in the Environment." *Chemosphere* 65 (5): 725–59. doi:10.1016/j.chemosphere.2006.03.026.

Sarri, Artemis K, Nikolaos C Megoulas, and Michael A Koupparis. 2006. "Development of a Novel Method Based on Liquid Chromatography-Evaporative Light Scattering Detection for the Direct Determination of Streptomycin and Dihydrostreptomycin in Raw Materials, Pharmaceutical Formulations, Culture Media and Plasma." *Journal of Chromatography. A* 1122 (1–2): 275–78. doi:10.1016/j.chroma.2006.06.001.

Sathish, M., B. Viswanathan, RP. Wiswanathan, and ChS. Gopinath. 2005. "Synthesis, Characterization, Electronic Structure, and Photocatalytic Activity of Nitrogen-Doped TiO2 Nanocatalyst." *Chemical Material* 17: 6349–53.

Senthilnathan, and Philip. 2010. "Photocatalytic Degradation of Lindane under UV and Visible Light Using N-Doped TiO2." *Chemical Engineering Journal* 161 (1–2): 83–92. doi:10.1016/j.cej.2010.04.034.

Shao, Gao-Song, Xue-Jun Zhang, and Zhong-Yong Yuan. 2008. "Preparation and Photocatalytic Activity of Hierarchically Mesoporous-Macroporous TiO2−xNx." *Applied Catalysis B: Environmental* 82 (3–4): 208–18. doi:10.1016/j.apcatb.2008.01.026.

Shi, Jian-Wen, Chang Liu, Chi He, Jun Li, Chong Xie, Shenghui Yang, Jian-Wei Chen, Shi Li, and Chunming Niu. 2015. "Carbon-Doped Titania Nanoplates with Exposed {001} Facets: Facile Synthesis{,} Characterization and Visible-Light Photocatalytic Performance." Article. *RSC Adv.* 5 (23). The Royal Society of Chemistry: 17667–75. doi:10.1039/C4RA15824E.

Shifu, Chen, Liu Xuqiang, Liu Yunzhang, and Cao Gengyu. 2007. "The Preparation of Nitrogen-Doped TiO2−xNx Photocatalyst Coated on Hollow Glass Microbeads." *Applied Surface Science* 253 (6): 3077–82. doi:10.1016/j.apsusc.2006.06.058.

Tetreault, Gerald R, Charles J Bennett, K Shires, B Knight, Mark R Servos, and Mark E McMaster. 2011. "Intersex and Reproductive Impairment of Wild Fish Exposed to Multiple Municipal Wastewater Discharges." *Aquatic Toxicology (Amsterdam, Netherlands)* 104 (3–4): 278–90. doi:10.1016/j.aquatox.2011.05.008.

Vaiano, V., O. Sacco, D. Sannino, and P. Ciambelli. 2014. "Photocatalytic Removal of Spiramycin from Wastewater under Visible Light with N-Doped TiO2 Photocatalysts." *Chemical Engineering Journal*, March. doi:10.1016/j.cej.2014.02.071.

Verlicchi, P., a. Galletti, M. Petrovic, and D. Barceló. 2010. "Hospital Effluents as a Source of Emerging Pollutants: An Overview of Micropollutants and Sustainable Treatment Options." *Journal of Hydrology* 389 (3–4). Elsevier B.V.: 416–28. doi:10.1016/j.jhydrol.2010.06.005.

Verlicchi, P, M Al Aukidy, and E Zambello. 2012. "Occurrence of Pharmaceutical Compounds in Urban Wastewater: Removal, Mass Load and Environmental Risk after a Secondary Treatment--a Review." *The Science of the Total Environment* 429 (July). Elsevier B.V.: 123–55. doi:10.1016/j.scitotenv.2012.04.028.

Vragović, Natalija, Davorin Bazulić, and Bela Njari. 2011. "Risk Assessment of Streptomycin and Tetracycline Residues in Meat and Milk on Croatian Market." *Food and Chemical Toxicology : An International Journal Published for the British Industrial Biological Research Association* 49 (2): 352–55. doi:10.1016/j.fct.2010.11.006.

Yoo, Jung Bo, Hyo Jin Yoo, Hyuk Joon Jung, Han Sol Kim, Sora Bang, Jongmyung Choi, Hoyoung Suh, Ji-Hyun Lee, Jin-Gyu Kim, and Nam Hwi Hur. 2016. "Titanium Oxynitride Microspheres with the Rock-Salt Structure for Use as Visible-Light Photocatalysts." *J. Mater. Chem. A* 0. Royal Society of Chemistry: 1–8. doi:10.1039/C5TA06758H.

Yun, Jung-Ho, Roong Jien Wong, Yun Hau Ng, Aijun Du, and Rose Amal. 2012.

"Combined Electrophoretic Deposition-Anodization Method to Fabricate Reduced Graphene Oxide-TiO2 Nanotube Films." Article. *RSC Adv.* 2 (21). The Royal Society of Chemistry: 8164–71. doi:10.1039/C2RA20827J.

Zaleska, A. 2008. "Doped-TiO2: A Review." *Recent Patents on Engineering*. file:///C:/Users/Cindy/Downloads/00b7d51e103e0c69cb000000.pdf.

Zarrabi, Mahshid, Mohammad H Entezari, and Elaheh K Goharshadi. 2015. "Photocatalytic Oxidative Desulfurization of Dibenzothiophene by C/TiO2@MCM-41 Nanoparticles under Visible Light and Mild Conditions." Article. *RSC Adv.* 5 (44). The Royal Society of Chemistry: 34652–62. doi:10.1039/C5RA02513C.

Zhang, Geshan, Yong Cai Zhang, Mallikarjuna Nadagouda, Changseok Han, Kevin O'Shea, Said M. El-Sheikh, Adel a. Ismail, and Dionysios D. Dionysiou. 2014. "Visible Light-Sensitized S, N and C Co-Doped Polymorphic TiO2 for Photocatalytic Destruction of Microcystin-LR." *Applied Catalysis B: Environmental* 144 (January). Elsevier B.V.: 614–21. doi:10.1016/j.apcatb.2013.07.058.

Zhang, Hanmin, Pengxiao Liu, Yujie Feng, and Fenglin Yang. 2013. "Fate of Antibiotics during Wastewater Treatment and Antibiotic Distribution in the Effluent-Receiving Waters of the Yellow Sea, Northern China." *Marine Pollution Bulletin* 73 (1). Elsevier Ltd: 282–90. doi:10.1016/j.marpolbul.2013.05.007.

Zhang, Zhaoguo, Zhengfeng Huang, Xudong Cheng, Qingli Wang, Yi Chen, Peimei Dong, and Xiwen Zhang. 2015. "Product Selectivity of Visible-Light Photocatalytic Reduction of Carbon Dioxide Using Titanium Dioxide Doped by Different Nitrogen-Sources." *Applied Surface Science* 355: 45–51. doi:10.1016/j.apsusc.2015.07.097.

Zuorro, Antonio, Roberto Lavecchia, Franco Medici, and Luigi Piga. 2013. "Spent Tea

Leaves as a Potential Low-Cost Adsorbent for the Removal of Azo Dyes from

Wastewater." In *Chemical Engineering Transactions*, 32:19–24. Italian Association of

Chemical Engineering - AIDIC. doi:10.3303/CET1332004.

Figure 1 XRD pattern of photocatalysts of Fe^{+3}-$TiO_{2-x}N_x$. (a) synthesis by sol-gel method;

(b) synthesis by microwave radiation.

Figure 2 Scanning electron micrography at different magnification of Fe^{+3}-$TiO_{2-x}N_x$

nanoparticles prepared by: (a-d) sol-gel method; (e-h) synthesis by microwave radiation.

Figure 3 Uv-Vis diffuse reflectance spectra of iron and nitrogen co-doped titanium dioxide

synthesized by sol-gel and microwave methods.

Figure 4 XPS spectra of N1s, O1s, Ti2p y Fe2p, from TNF-MW nanoparticle.

Figure 5 XPS spectra of N1s, O1s, Ti2p y Fe2p, from TNF-SG nanoparticle.

Figure 6 Removal efficiency of AMX at different pH values, using Fe^{+3}-$TiO_{2-x}N_x$

nanoparticles synthesized by sol-gel method as catalyst. [a] particles size was calculated by

Scherrer equation.

Figure 7 Comparison of degradation of amoxicillin (AMX deg.) at different pH values (3.5, 7 and 9.5), using Fe^{+3}-$TiO_{2-x}N_x$ nanoparticles synthesized by microwave radiation as catalyst.

Figure 8 Comparison of degradation of STR (STR deg.) at different pH values (3.5, 7 and 8), using Fe^{+3}-$TiO_{2-x}N_x$ nanoparticles synthesized by sol-gel method as catalyst.

Figure 9 Comparison of degradation of amoxicillin STR at different pH values, using Fe^{+3}-$TiO_{2-x}N_x$ nanoparticles synthesized by microwave radiation as catalyst.
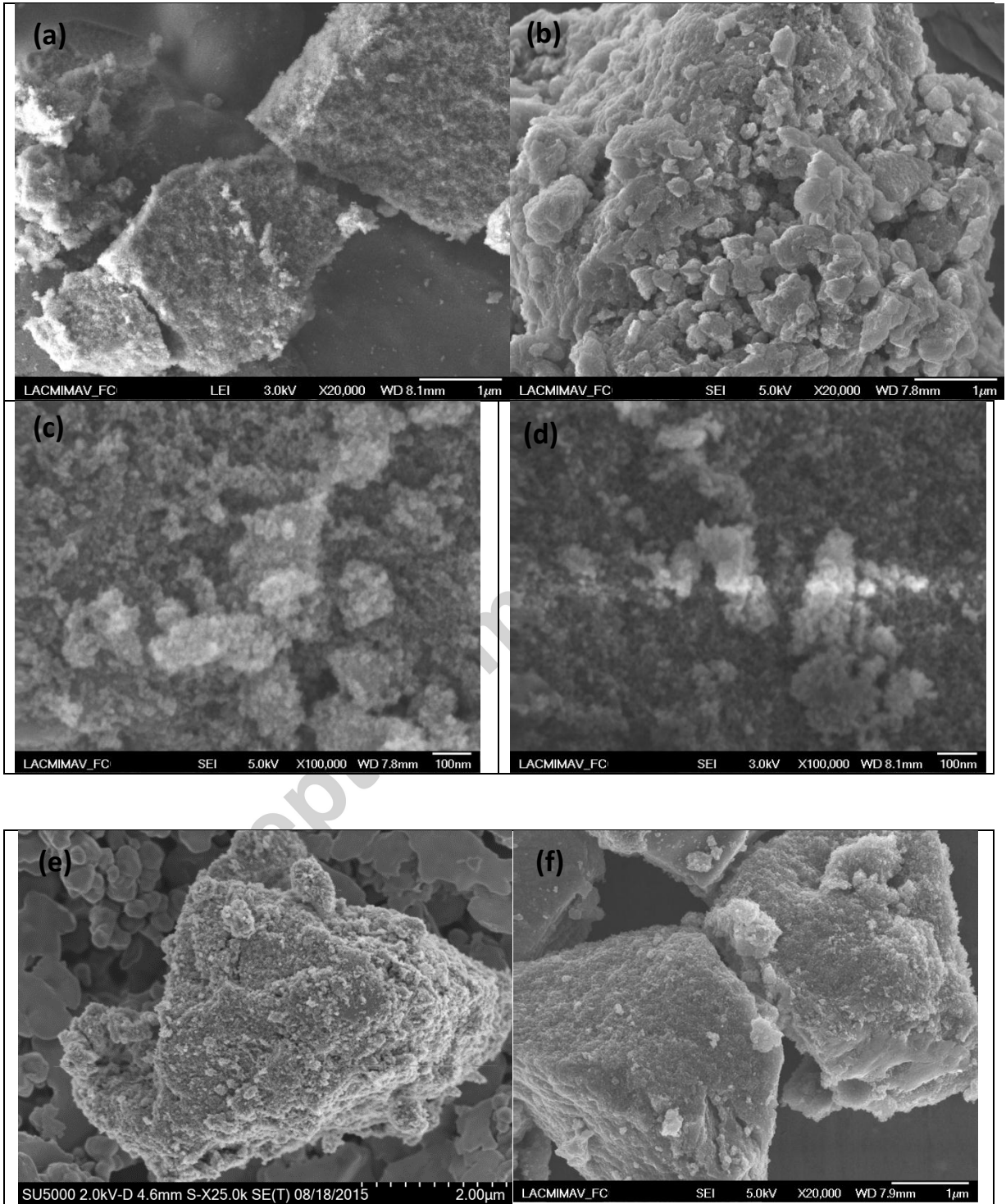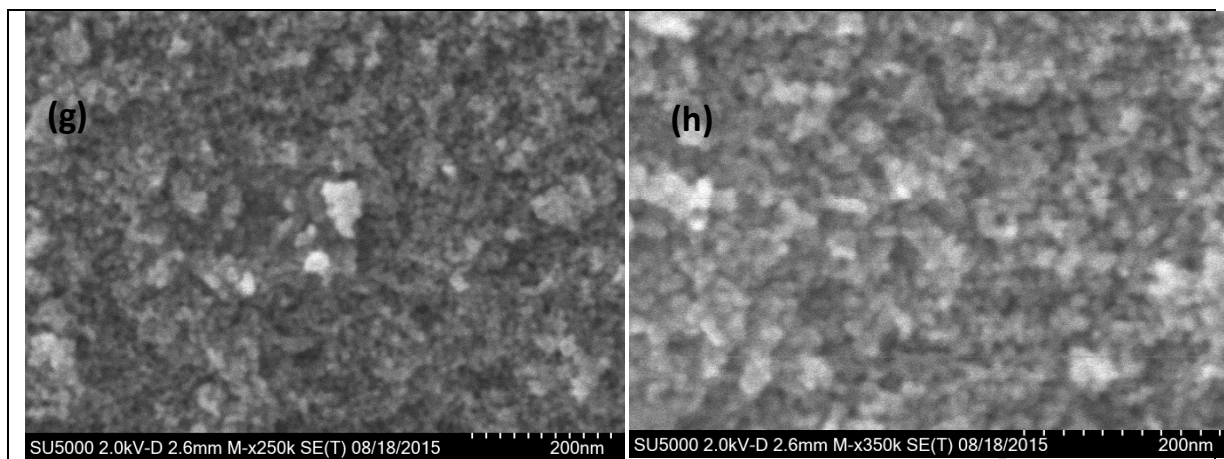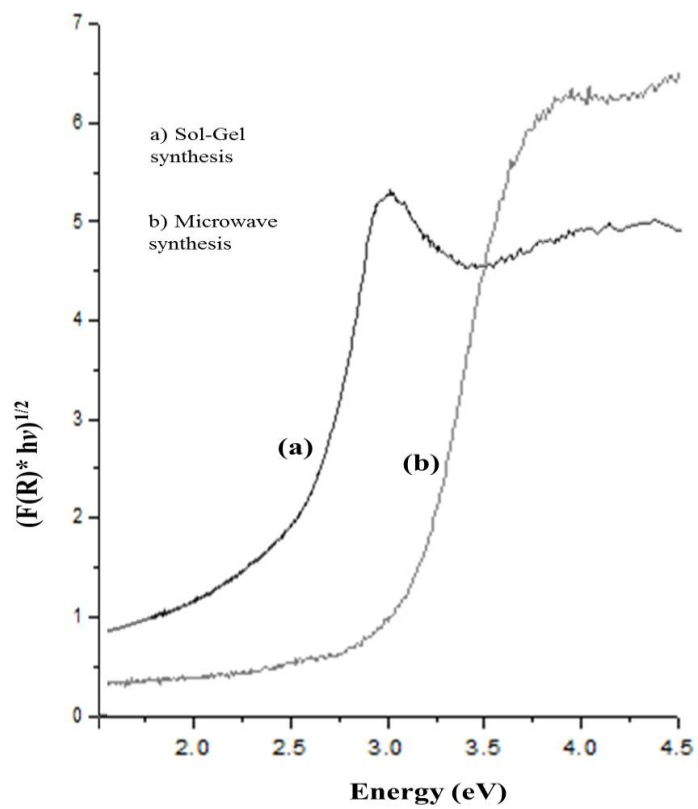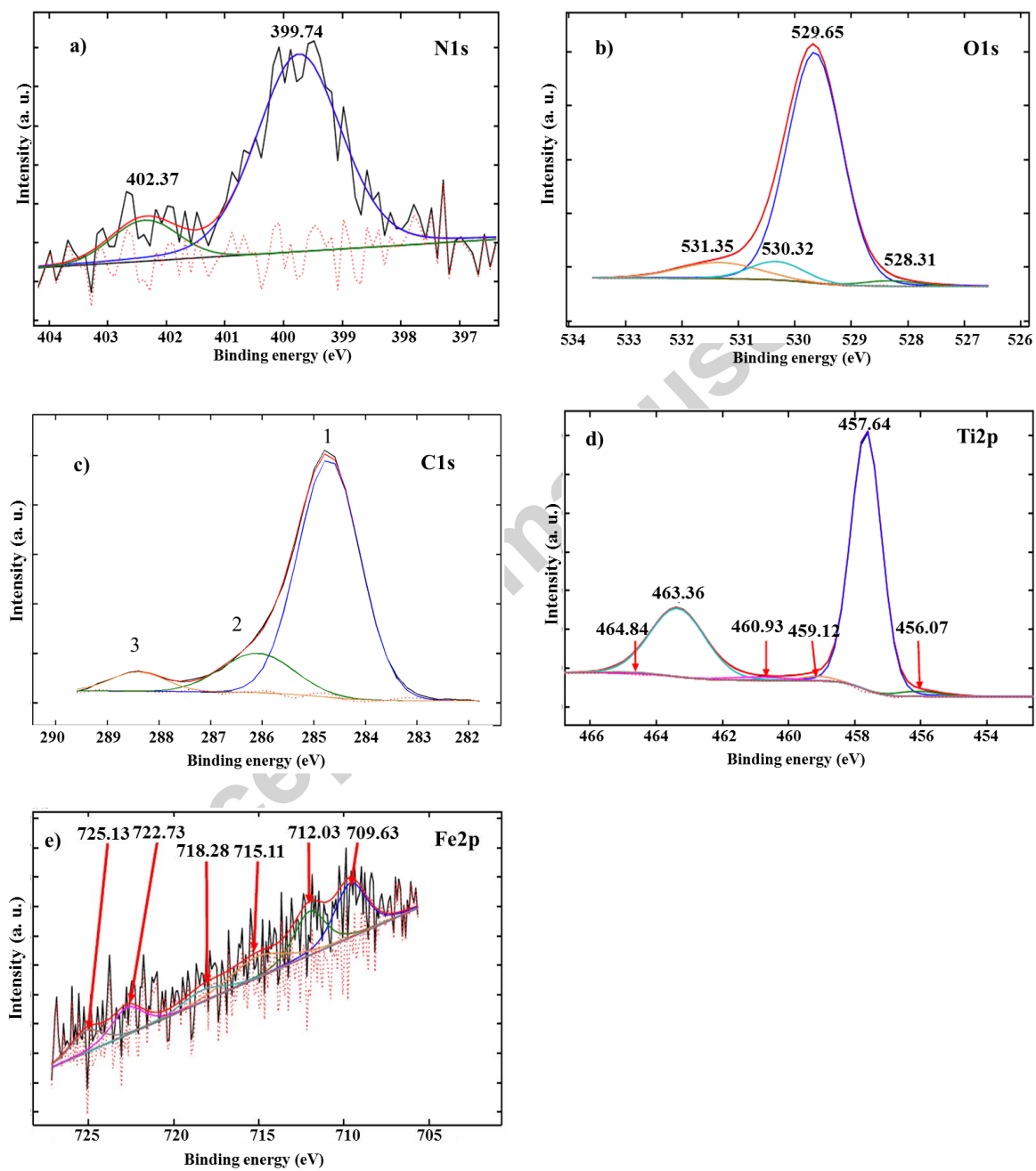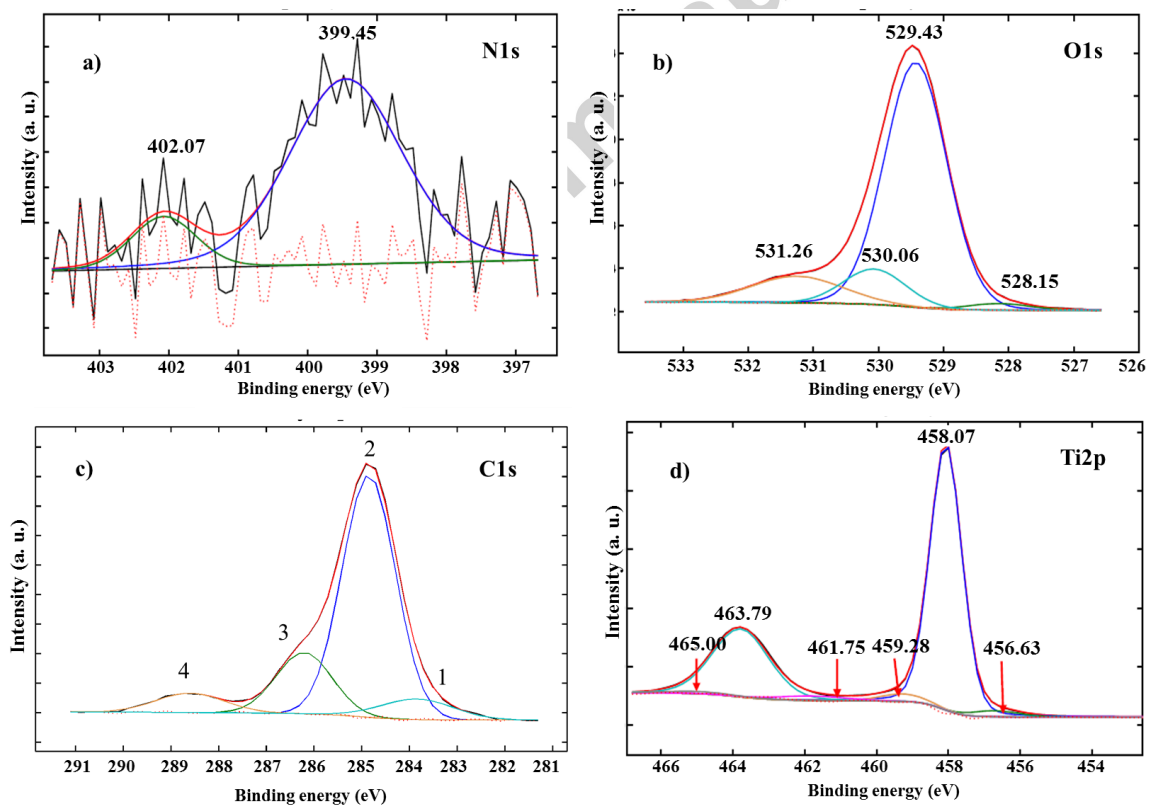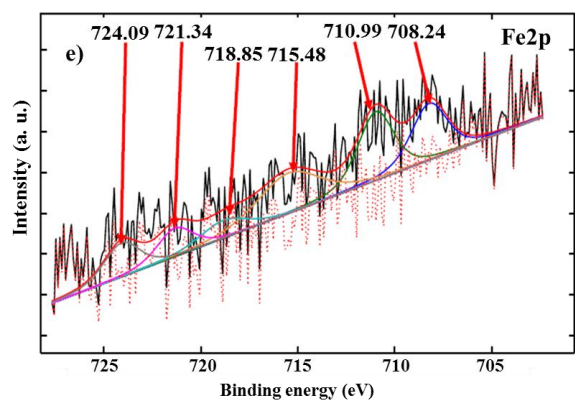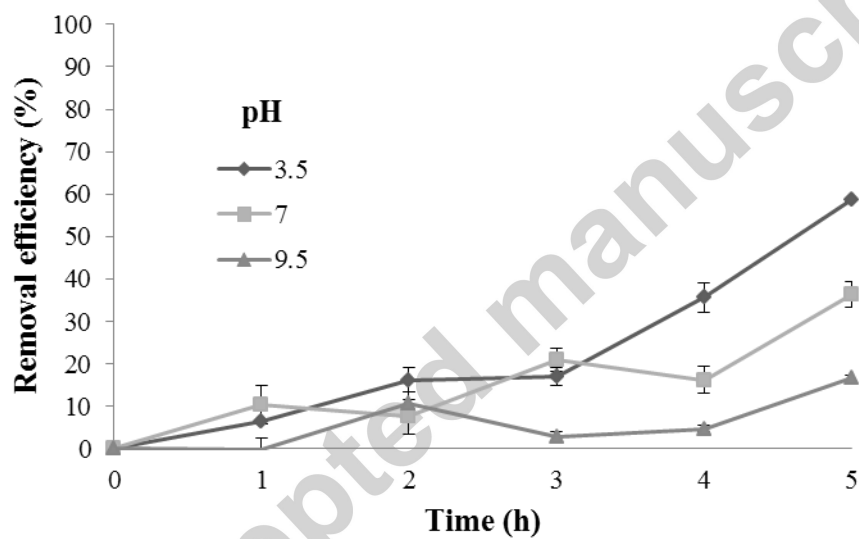
Figure 1
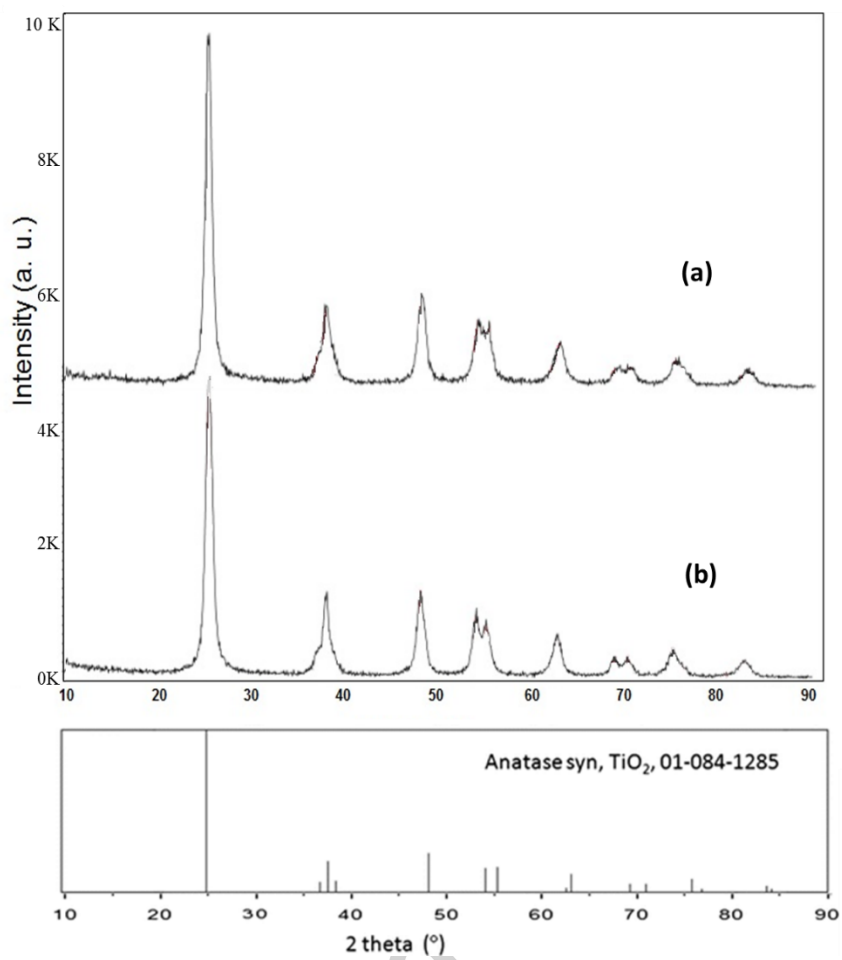
Figure 2
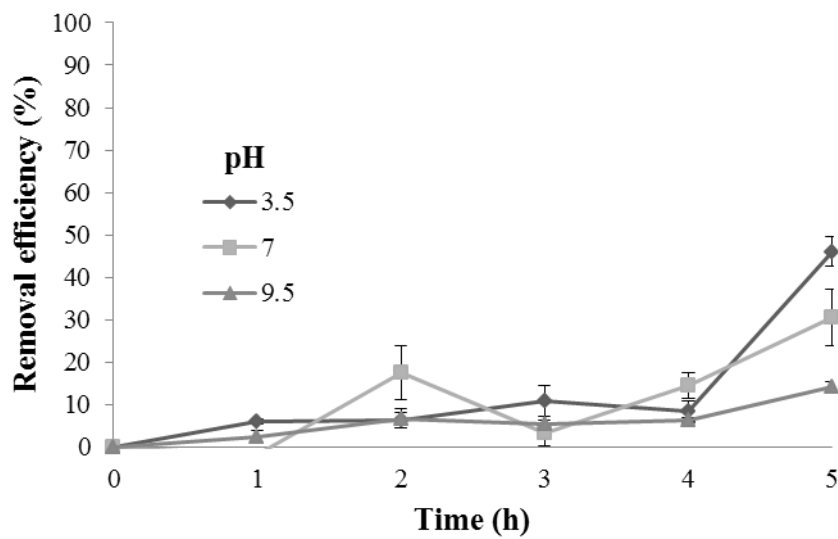
Figure 3

Figure 4

Figure 5

Figure 6

Figure 7

Figure 8
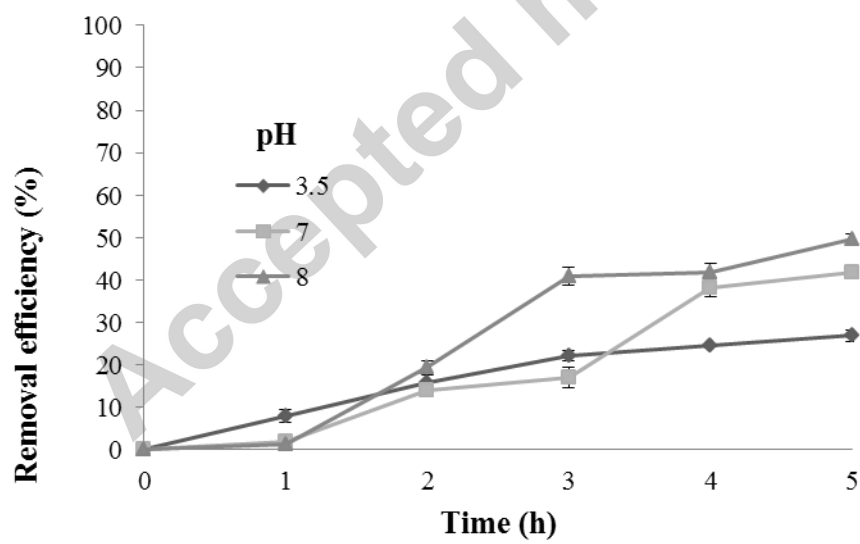
Figure 9
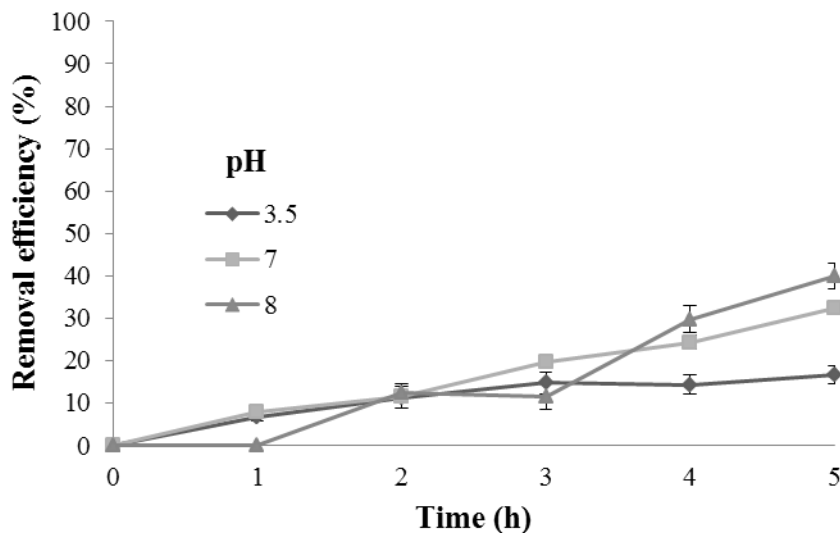
Table 1 Some representative examples of TiO_2 and TiO_2-N materials .

Material	Preparation	Properties	Application	Reference
$TiO_{2-x}N_x$	Sol gel processes, hydrothermal treatment, supercritical methods, sputtering techniques, TiN oxidation	Visible light active materials with different morphologies and topologies	Environmental and energy-related applications: photocatalysis, dye-sensitized solar cells, lithium-ion batteries, electrochromic displays	Bakar and Ribeiro, **2016**
$TiO_{2-x}N_x$	Hydrothermal	Brookite $TiO_{2-x}N_x$ nanorods, visible light	Rhodamine B photodegradation	Pan and Jiang, **2016**

		active		
$TiO_{2-x}N_x$	Hydrothermal	Thin films, nanorod arrays, visible light active	Photocatalytic oxidation of CO_2	Z. Zhang et al. **2015**
$N-TiO_2$ and N-codoped-TiO_2	Oxidation of TiN, Mechanochemical method, sol-gel, sputtering, Atomic Layer Deposition, Chemical Vapor Deposition	Visible light active materials, enhanced phtotocatalytic activity, powders, films	Photooxidation of Volatile organic Compounds; Water splitting; antibacterial, antiviral and antiallergen properties; slef-cleaning; Tooth bleaching, air purification systems, water treatment systems	Asahi R et al **2014**
$N-TiO_2$ supported on strontium ferrite	Hydrothermal	Magnetic properties, visible light activity	Degradation of the pesticide: 2,4-Dichlorophenol	Aziz et al. **2012**
TiO_2 P25	Comercial P25	-	Degradation of antibiotics	Dimitrakopoulou et al. **2012**
TiO_2 and $CuO/TiO_2/Al_2O_3$	Electrophoresis	EDAX y DRX.	Degradation of paracetamol	Arredondo Valdez et al. **2012**
$Mo-N-TiO_2$	Hydrolysis-Precipitation method	Anatase and rutile crystalline phases, visible light active materials	Photocatalysis: degradation of phenol	Cheng et al. **2012a**

TiO_2	Anodic oxidation on Ti sheet.	SEM, XRD	Degradation of triclosan	Liu and Syu, **2013**
TiO_2	Comercial P25	-	Degradation of tetracycline	Zhu et al. **2013**
$ClTiO_2$	Microwave-assisted synthesis.	XPS, XRD, UV-Vis DRS, FT-IR, TEM and SEM	Degradation of tetracycline	Liu X. et al. **2013**
TiO_2	Comercial P25	-	Degradation of antibiotics	Nasuhoglu et al. **2012**

Table 2 Physicochemical properties of TiO_2, Fe^{3+}-TiO_2 and TiO_2-N nanostructured powders: [A] Catalyst synthesized by sol-gel; [B] Catalyst synthesized by microwave method.

Catalyst	Crystallite size (nm)[a]	E_g (mV)	SSA (m^2 g^{-1})
TiO_2[1]	12.69	3.08	110.7
TiO_2-Fe 1 % [1]	8.95	2.71	177.3
TiO_2-N [2]	20.00	3.00	41.00
TiO_2 -Fe, N [3]	9.4	2.53	133
Fe^{+3}-$TiO_{2-x}N_x$ [A]	7.72	2.53	103.1
Fe^{+3}-$TiO_{2-x}N_x$ [B]	7.09	3.00	135.3
TiO_2-Fe 0.5 % [A]	10.61	2.69	-
TiO_2-Fe 0.5 % [B]	9.45	3.06	-
TiO_2-N 10 % [A]	9.55	3.05	-
TiO_2-N 10 % [B]	9.47	3.08	-

Table 3 DLS analysis of the prepared materials.

Material	pH	Zeta Potential (mV)	Size (nm)

MW	3.5	-27.47	472
MW	7	-6.69	640
MW	8	+2.80	752
MW	9.5	+26.14	427
SG	3.5	+30.41	457
SG	7	-32.16	455
SG	8	-32.46	460
SG	9.5	-37.89	300

Table 4. XPS analysis of Fe^{3+}-TiO_2,N,C materials. A comparison on the elemental composition (and chemical speciation) of the SG and MW materials is presented.

	Fe^{+3}-$TiO_{2-x}N_x$ SG				Fe^{+3}-$TiO_{2-x}N_x$ MW		
Element	% Átomic	Species	Oxidation state	Element	% Átomic	Species	Oxidation state
O1s	49.0	O-Ti-O-N	O^{2-}	O1s	53.3	O-Ti-O-N	O^{2-}
		O-Ti-O	O^{2-}			O-Ti-O	O^{2-}
		C=O/C-OH	O^{2-}			C=O/C-OH	O^{2-}
Ti2p	18.0	Ti-O-N	Ti^{3+}	Ti2p	24.1	Ti-O-N	Ti^{3+}
		Ti-O	Ti^{4+}			Ti-O	Ti^{4+}
		O-Ti-O	Ti^{4+}			O-Ti-O	Ti^{4+}
C1s	25.8	C-C		C1s	12.8	O-Ti-C	
		C-O, C=C, C=O				C-C	
		Ti-O-C=O				C-O, C=C, C=O	
						Ti-O-C=O	
N1s	0.5	Ti-O-N/N-Ti-O		N1s	0.6	Ti-O-N/N-Ti-O	
		N-H	N^{3-}			N-H	N^{3-}
Fe2p3	0.7	Fe-O	Fe^{3+} / Fe^{2+}	Fe2p3	0.2	Fe-O	Fe^{3+} / Fe^{2+}

Table 5. Comparison on the degradation efficiencies of amoxicillin and streptomycin after 5 hours of photocatalytic treatment under visible light, using the catalysts synthesized by the sol-gel (SG) and microwave radiation method (MW), at different pH values.

Antibiotic	pH	Degradation %		Mineralization %	
		SG	MW	SG	MW
Amoxicillin	3.5	58.61	46.12	41.51	35.99
	7	32.29	30.56	25.76	15.62
	9.5	16.60	14.13	0.00	0.00
Streptomycin	3.5	26.80	16.63	25.85	3.50
	7	41.80	32.47	24.64	18.30
	8	49.67	39.9	34.72	29.86